Science Advances
AAAS

Supplementary Materials for

Formation of the elusive tetrahedral P_3N molecule

Chaojiang Zhang *et al.*

Corresponding author: André K. Eckhardt, andre.eckhardt@rub.de; Ralf I. Kaiser, ralfk@hawaii.edu

Sci. Adv. **8**, eabo5792 (2022)
DOI: 10.1126/sciadv.abo5792

This PDF file includes:

Error determination of computed ionization energies
Figs. S1 to S4
Tables S1 to S9
References

Error determination of computed ionization energies

As the identification of different isomers in our studies focuses on the ionization energy of each isomer, we also performed additional ionization energy computations at the CCSD(T)/CBS//B3LYP/cc−pVTZ level of theory for multiple nitrogen- and phosphorus-containing molecules as benchmarks (Table S1). The adiabatic ionization energies (IEs) were computed by taking the zero-point vibrational energy corrected energy difference between the neutral and ionic species that correspond to similar conformations. Error bounds were determined by subtracting the calculated ionization energy from the error boundaries of the experimentally determined and hence known values for each molecule. Afterward, the average difference to the lower and upper boundary as well as their standard deviation was calculated. Finally, the standard deviation was subtracted from or added to the average difference for the lower and upper boundary, respectively. This conservative analysis yielded errors of −0.08/+0.07 eV, which allows us to distinguish all isomers of interest in this study based on their calculated and/or experimentally determined ionization energy.

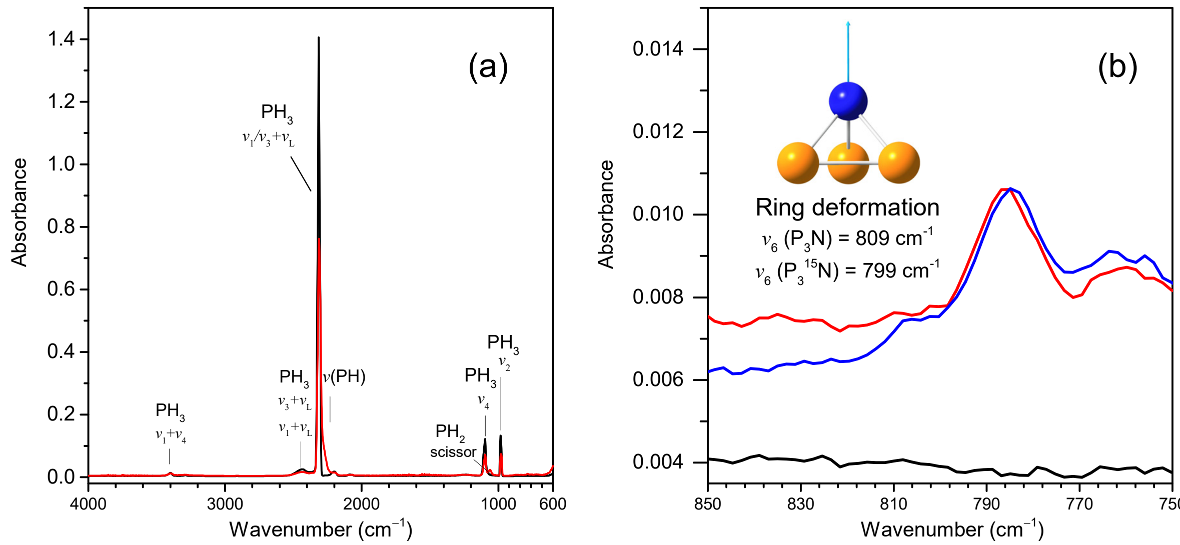

Fig. S1. Fourier−transform infrared spectroscopy (FTIR) spectra of the phosphine (PH_3) + nitrogen (N_2) ice before (black) and after (red) processing with energetic electrons. (a) FTIR spectra between 600 to 4000 cm^{-1}. (b) FTIR spectra between 750 to 850 cm^{-1}. The blue line is from the irradiated PH_3 + $^{15}N_2$ ice mixtures. The peak at 788 cm^{-1} of energetic electrons irradiated PH_3 + N_2 ice can be linked to the P-N ring deformation (v_6), which was calculated to be 809 cm^{-1} at the B3LYP/cc-pVTZ level of theory. The replacement of nitrogen by 15–nitrogen (^{15}N) shifts the 788 cm^{-1} feature to 784 cm^{-1}. The calculated vibration energy of ring deformation (v_6) of $P_3{}^{15}N$ is 799 cm^{-1}, lower than that of P_3N, which is in agreement with experimental observation. However, since the electron exposure synthesizes a wide range of new molecules and other molecules such as prismatic P_3N_3 also have absorption at 824 cm^{-1} (reference 29). It is cannot be exploited to unambiguously assign the peak at 788 cm^{-1} is from P_3N.

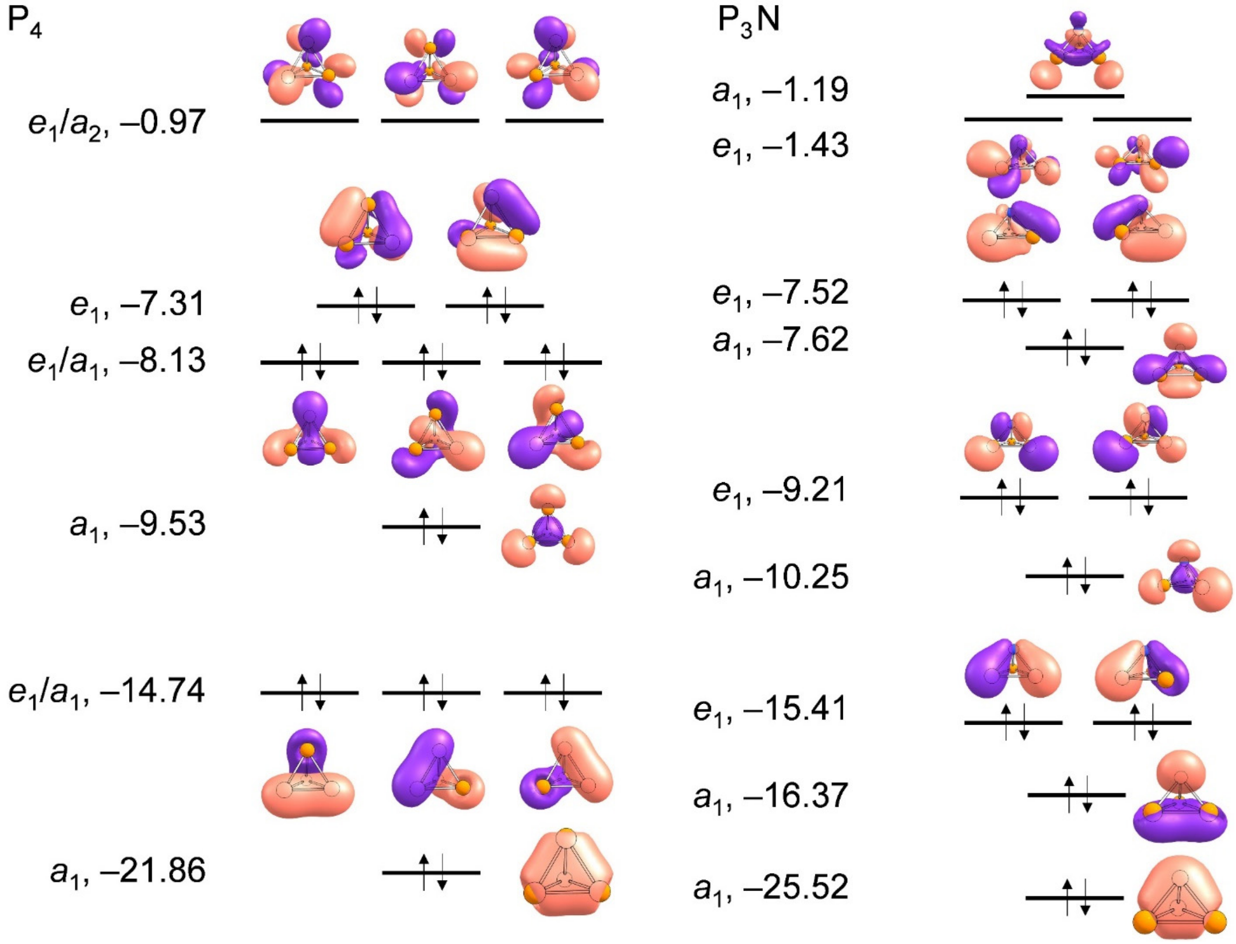

Fig. S2. Molecular orbitals diagrams for P_4 (right) and P_3N (right) calculated at B3LYP/cc−PVTZ level of theory. Both diagrams were calculated using C_{3v} symmetry to allow for direct comparison of the calculated orbitals.

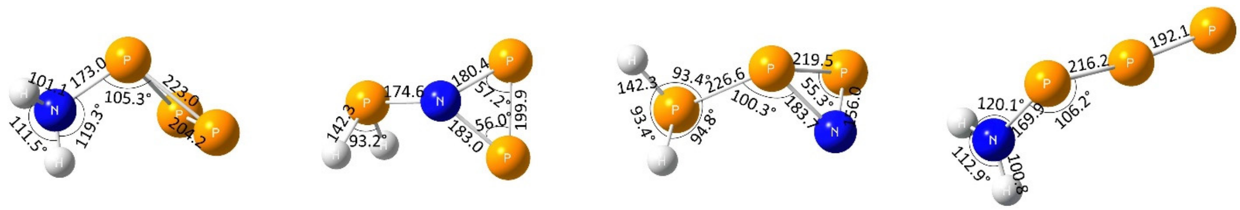

13, C_1, ^{1}A
8.21 – 8.36 eV
0.0 kJ mol^{-1}

14, C_1, ^{1}A
7.67 – 7.82 eV
+160.2 kJ mol^{-1}

15, C_1, ^{1}A
8.44 – 8.59 eV
+132.6 kJ mol^{-1}

16, C_s, ^{1}A'
6.51 – 6.66 eV
+163.6 kJ mol^{-1}

Fig. S3. Molecular structure of H_2P_3N isomers. Bond length in picometers (pm), bond angle in degree, point groups, ground states, computed adiabatic ionization energies corrected for the electric field effect (Stark effect) and computational errors (blue), and relative energies (red) are also shown. The energies were computed at the CCSD(T)/CBS//B3LYP/cc−pVTZ level of theory. The atoms are color coded in white (hydrogen), blue (nitrogen), and orange (phosphorus).

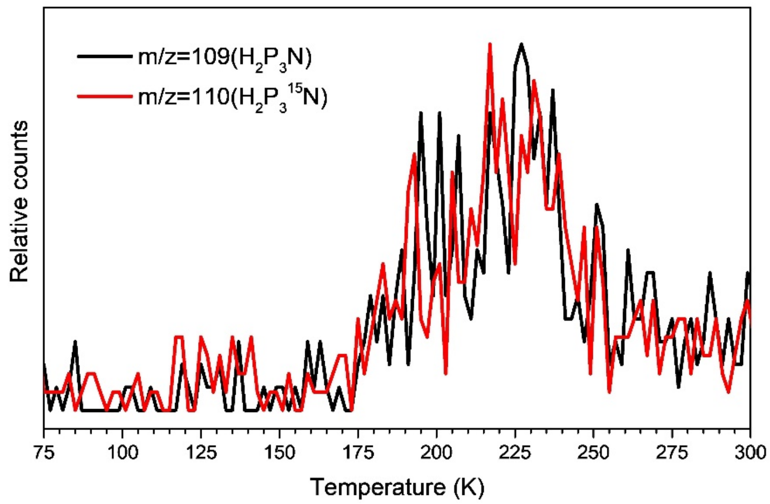

Fig. S4. Temperature programmed desorption (TPD) profile of H_2P_3N from the electron processed phosphine (PH_3)–nitrogen (N_2) and phosphine (PH_3)–15–nitrogen ($^{15}N_2$) ices via photoionization reflectron time-of-flight mass spectrometry (PI–ReTOF–MS) at a photon energy of 10.49 eV. The shift of the TPD profile from m/z = 109 to m/z = 110 in the temperature range from 175 K to 300 K reveals that the molecule of interest carries a single nitrogen atom.

Table S1. Computed adiabatic ionization energies (IEs) of distinct P_3N isomers along with error limits and previous computational (CCSD(T)/CBS//B3LYP/cc–pVTZ plus zero-point vibrational energy (ZPVE) corrections) and experimental benchmarks of different nitrogen- and phosphorus-containing compounds. An offset of 0.03 eV was subtracted to correct for the electric field effect.

Compounds	Experimental IE (eV)	Experimental Error Limits (eV)	Computed IE (eV)	Computed IE– Experimental IE (max) (eV)	Computed IE– Experimental IE (min) (eV)	IE range after error analysis (eV)	Corrected IE with electric field effect (eV)
Ammonia NH_3	10.07 ± 0.02	10.05 – 10.09 (*57*)	10.15	+0.06	+0.10		
Phosphine PH_3	9.869 ± 0.002	9.867 – 9.871 (*57*)	9.82	–0.051	–0.047		
Hydrogen cyanide HCN	13.60 ± 0.01	13.59 – 13.61 (*57*)	13.57	–0.04	–0.02		
Methinophosphide HCP	10.79 ± 0.01	10.78 – 10.80 (*58*)	10.76	–0.04	–0.02		
Acetonitrile CH_3CN	12.20 ± 0.01	12.19 – 12.21 (*59*)	12.20	–0.01	+0.01		
Methyl Isocyanide CH_3NC	11.24 ± 0.01	11.23 – 11.25 (*59*)	11.25	+0.00	+0.02		
2H-Azirine *c*-H_2CCHN	10.05 ± 0.03	10.02 – 10.08 (*59*)	10.02	–0.06	+0.00		
P_3N **10**			9.44			9.36 – 9.51	9.33 – 9.48
P_3N **11**			8.42			8.34 – 8.49	8.31 – 8.46
P_3N **12**			7.94			7.86 – 8.01	7.83 – 7.98
				Average –0.04 ± 0.04	Average 0.02 ± 0.05		
				Error Limits –0.08 – +0.00	Error Limits –0.02 – +0.07		
				Combined Error Limits –0.08 – +0.07			

Table S2. Infrared absorption peaks before and after irradiation for phosphine (PH_3) + nitrogen (N_2)/15–nitrogen ($^{15}N_2$) ices.

Pristine ice, before irradiation (5 K)		
Assignment	Position with ^{14}N (cm^{-1})	Position with ^{15}N (cm^{-1})
PH_3 (ν_2)	983	982
PH_3 (ν_4)	1098	1098
PH_3 ($\nu_{2+}\nu_4$)	2074, 2087	2075, 2089
PH_3 ($2\nu_4$)	2199	2200
PH_3 (ν_1/ν_3)	2314	2315
PH_3 ($\nu_1/\nu_{3+}\nu_L$)	2435	2435
PH_3 ($\nu_{1+}\nu_4$)	3398	3399
New peaks after irradiation (5 K)		
ν (P–N)	788	784
ν (PH_2)	1063	1063
ν (PH)	2270	2270

Table S3. Data used to calculate the average irradiation dose per molecule.

Initial kinetic energy of the electrons, E_{init} (keV)		5
Ice		$PH_3 + N_2$
Irradiation current, I (nA)		100 ± 5
Total number of electrons		$(4.5 \pm 0.5) \times 10^{15}$
Average penetration depth, l_{ave} (nm)[a]		490 ± 50
Maximum penetration depth, l_{max} (nm)[a]		880 ± 90
Average kinetic energy of backscattered electrons, E_{bs} (keV)[a]		2.96 ± 0.30
Fraction of backscattered electrons, f_{bs}[a]		0.12 ± 0.01
Average kinetic energy of transmitted electrons, E_{trans} (keV)[a]		0
Fraction of transmitted electrons, f_{trans}[a]		0
Irradiated area, A (cm^2)		1.0 ± 0.1
Dose (eV/molecule)	PH_3	26 ± 4
	N_2	21 ± 3

Note:

[a] Parameters obtained using the CASINO software v2.42.

Table S4. Parameters for the vacuum ultraviolet (VUV) light generation used in the present experiments.[a]

$2\omega_1 - \omega_2$	Photoionization energy (eV)	10.49 ($3\omega_1$)	8.53
	Flux (10^{11} photons s^{-1})	12 ± 1	10 ± 1
	Wavelength (nm)	118.222	145.351
ω_1	Wavelength (nm)	355	202.316
Nd:YAG (YAG A)	Wavelength (nm)	355	532
Dye laser (DYE A)	Wavelength (nm)	-	606.948
Dye		-	Rhodamine 610 and 640
ω_2	Wavelength (nm)	-	332.5
Nd:YAG (YAG B)	Wavelength (nm)	-	532
Dye laser (DYE B)	Wavelength (nm)	-	665
Dye		-	DCM
	Nonlinear medium	Xe	Kr

Note:

[a] The uncertainty for VUV photon energies is 0.001 nm.

Table S5. Cartesian Coordinates (distances in Å), vibrational frequencies (cm^{-1}), and intensity (km mol^{-1}) for selected structures of P_3N.

P_3N

10

N	0.000000	–0.000000	–1.144000
P	0.625874	–1.084046	0.181489
P	0.625874	1.084046	0.181489
P	–1.251748	–0.000000	0.181489

Frequency/ cm^{-1}	Intensity/ km mol^{-1}
444.4492	1.3595
444.4496	1.3608
544.2406	0.1029
544.2422	0.1030
573.7471	9.1367
809.6134	14.8447

11

P	0.403272	0.092766	–1.149072
N	1.393737	–0.628589	–0.000000
P	–1.436646	0.098649	0.000000
P	0.403272	0.092766	1.149072

Frequency/ cm^{-1}	Intensity/ km mol^{-1}
280.2042	16.4727
356.2358	5.5564
465.2703	2.6853
542.8618	24.2115
685.3898	6.5155
871.8844	56.0624

12

N	–0.817775	0.502928	0.000000
P	–0.388189	–0.023629	–1.522971
P	–0.388189	–0.023629	1.522971
P	1.146090	–0.180113	–0.000000

Frequency/ cm^{-1}	Intensity/ km mol^{-1}
284.9089	13.7429
391.2465	1.4913
409.2017	2.4952
474.3462	29.529
689.4443	27.8686
938.2833	39.6746

Table S6. Cartesian Coordinates (distances in Å), vibrational frequencies (cm^{-1}), and intensity (km mol^{-1}) for selected structures of H_2P_3N.

H_2P_3N

13

N	1.915443	0.069833	0.629383
P	0.799638	–0.009703	–0.689723
P	–1.012468	–1.015369	0.132954
P	–0.974084	1.025931	0.129013
H	2.805729	–0.372230	0.445472
H	1.589868	–0.129475	1.565195

Frequency/ cm^{-1}	Intensity/ km mol^{-1}
164.7569	10.5528
228.0706	2.0497
246.4608	9.0604
397.5159	2.0754
442.0217	65.0478
481.4911	147.1390
637.2915	1.2766
777.2271	62.4324
956.8749	3.5827
1580.4995	36.1624
3510.6820	12.5457
3618.0470	22.4603

14

P	–1.811571	0.112326	–0.094567
N	–0.236936	0.018824	0.654248
P	1.092883	–1.006969	–0.071587
P	1.092341	0.991688	–0.080787
H	–2.359973	–1.064983	0.486415
H	–1.586265	–0.522449	–1.362031

Frequency/ cm^{-1}	Intensity/ km mol^{-1}
155.0673	4.9424
181.7655	2.9263
217.8146	2.2195
364.2540	3.3784
498.7113	13.7236
682.6416	12.2584
848.5154	76.2553
892.7777	41.6065
945.5286	27.3889
1116.8445	29.7094
2269.6257	84.1787
2361.2527	73.8892

15

P	1.889758	0.317965	0.984491
P	0.457531	–0.540514	–0.547380
N	–1.135879	–0.335996	0.343337
P	–1.104387	1.000963	–0.526925
H	3.040926	0.005141	0.208072
H	1.976178	–0.878573	1.750700

Frequency/ cm^{-1}	Intensity/ km mol^{-1}
46.5454	2.7108
148.1121	2.0689
226.2145	4.1758
408.5688	7.0950
449.2837	7.3841
551.8420	6.5222
700.8081	8.2440
729.3840	5.7233
1061.8910	11.7423
1092.6631	16.1759
2361.5044	35.2288
2373.3769	44.2128

16

N	0.746238	–2.464836	0.000000
P	–0.661147	–1.513714	0.000000
P	0.000000	0.544509	0.000000
P	0.140015	2.459915	0.000000
H	1.296661	–2.553394	0.840353
H	1.296661	–2.553394	–0.840353

Frequency/ cm^{-1}	Intensity/ km mol^{-1}
17.5494	0.3811
29.4234	2.7068
219.2359	12.5258
345.3853	11.4658
408.4469	12.7099
461.4909	202.7951
754.0716	27.0566
837.4908	81.7484
929.2109	2.5060
1588.2163	17.7973
3533.3944	20.0334
3633.9684	35.3072

Table S7. Cartesian Coordinates (distances in Å) and CBS–QB3 energies (Hartrees) for all structures depicted in Fig. 4.

N_2H_4

N	0.000000	0.717816	–0.075902
N	–0.000000	–0.717816	–0.075902
H	0.230092	1.098141	0.836948
H	–0.937290	1.020386	–0.305636
H	–0.230092	–1.098141	0.836948
H	0.937290	–1.020386	–0.305636

E(CBS-QB3) = –111.680378

P_2H_4

P	0.000000	–1.130729	0.000000
P	–0.000000	1.130728	–0.000000
H	–0.981428	1.224954	1.026204
H	–0.981428	1.224954	–1.026204
H	0.981434	–1.224947	1.026200
H	0.981434	–1.224947	–1.026200

E(CBS-QB3) = –684.185215

NPH_4

N	1.111257	0.042491	0.079480
P	–0.600492	–0.124139	0.026088
H	1.540829	0.843038	–0.359016
H	1.604230	–0.803660	–0.158457
H	–0.964191	0.497525	–1.211574
H	–0.952284	1.027752	0.781361

E(CBS-QB3) = –397.956748

N_4 E(CBS-QB3) = –218.508006

P_4 E(CBS-QB3) = –1363.722909

P_3N E(CBS-QB3) = –1077.427727

$P(PH_2)_3$

P	–0.000000	–0.000000	0.799840
P	0.000000	2.007913	–0.188351
P	1.738904	–1.003957	–0.188351
P	–1.738904	–1.003957	–0.188351
H	–1.442746	–2.307820	0.295909
H	–1.169992	–1.245804	–1.469847
H	–1.277258	2.403364	0.295909
H	–0.493902	1.636144	–1.469847
H	2.720004	–0.095545	0.295909
H	1.663894	–0.390341	–1.469847

E(CBS-QB3) = –1367.215597

$N(PH_2)_3$

N	–2.832244	2.230896	0.404722
P	–1.110743	1.965808	0.407468
P	–3.697306	3.082679	–0.846112
P	–3.689536	1.574459	1.775711
H	–4.768636	0.927564	1.106101
H	–4.498470	2.695739	2.121499
H	–0.677567	3.284806	0.076856
H	–0.947453	1.520167	–0.938438
H	–3.118494	2.457114	–1.991084
H	–2.848643	4.223089	–0.975144

E(CBS-QB3) = –1080.969464

$N(NH_2)_3$

N	–0.000000	–0.000000	0.397743
N	0.000000	1.352030	–0.056639
N	1.170892	–0.676015	–0.056639
N	–1.170892	–0.676015	–0.056639
H	–0.700574	1.834697	0.495253
H	–0.328402	1.386540	–1.026847
H	–1.238607	–1.524063	0.495253
H	–1.036578	–0.977674	–1.026847
H	1.939181	–0.310634	0.495253
H	1.364980	–0.408866	–1.026847

E(CBS-QB3) = –222.169027

$P(PH_2)_2(NH_2)$

P	–2.977255	1.750425	–0.225685
N	–1.285876	1.903698	0.064023
P	–3.773492	3.718965	–1.011195
P	–3.642240	2.094578	1.894922
H	–3.577724	0.722993	2.261799
H	–5.028779	2.042508	1.587575
H	–3.030794	3.648137	–2.220459
H	–2.836690	4.577910	–0.370250
H	–0.935848	2.780106	0.428353
H	–0.713694	1.579990	–0.702624

E(CBS-QB3) = –1080.986122

Table S8. Calculated NICS values and orbital energies of the a_1 (s, π) orbital.

	NICS (center of tetrahedron)	NICS (center of trigons in tetrahedron)				a_1 / eV
		PPP	PPN	PNN	NNN	
P_4	–61.3	–59.8	–	–	–	–8.13
P_3N	–73.7	–55.9	–61.7	–	–	–7.62
P_2N_2	–64.6	–	–59.2	–65.9	–	–7.67
PN_3	–57.6	–	–	–64.5	–75.5	–10.82
N_4	–73.8	–	–	–	–73.2	–11.28

Table S9. Calculated standard reaction enthalpies and Gibbs free energies at 298 K at the CBS–QB3//B3LYP/cc–pVTZ level of theory.

Reactant	Products	ΔH_r^0 / kJ mol^{-1}	ΔG_r^0 / kJ mol^{-1}
P_4	2 P_2	236.0	189.7
P_3N	P_2 + PN	122.1	77.9
P_2N_2	2 PN	–8.9	–53.6
P_2N_2	P_2 + N_2	–224.7	–265.7
PN_3	PN + N_2	–373.4	–416.9
N_4	2 N_2	–740.6	–785.4

REFERENCES AND NOTES

1. F. Krafft, Phosphorus. From elemental light to chemical element. *Angew. Chem. Int. Ed.* **8**, 660–671 (1969).

2. L. R. Maxwell, S. B. Hendricks, V. M. Mosley, Electron diffraction by gases. *J. Chem. Phys.* **3**, 699–709 (1935).

3. M. T. Nguyen, T. L. Nguyen, A. M. Mebel, R. Flammang, Azido-nitrene is probably the N_4 molecule observed in mass spectrometric experiments. *J. Phys. Chem. A* **107**, 5452–5460 (2003).

4. A. Bettendorff, Allotropische zustände des arsens. *Justus Liebigs Ann. Chem.* **144**, 110–114 (1867).

5. Y. Morino, T. Ukaji, T. Ito, Molecular structure determination by gas electron diffraction at high temperatures. I. Arsenic. *Bull. Chem. Soc. Jpn.* **39**, 64–71 (1966).

6. G. M. Rosenblatt, The composition of antimony vapor. *J. Phys. Chem.* **66**, 2259–2260 (1962).

7. T. A. Engesser, W. J. Transue, P. Weis, C. C. Cummins, I. Krossing, As–P vs. P–P insertion in AsP_3: Kinetic control of the formation of $[AsP_3NO]^+$. *Eur. J. Inorg. Chem.* **2019**, 2607–2612 (2019).

8. P. Weis, D. C. Rohner, R. Prediger, B. Butschke, H. Scherer, S. Weber, I. Krossing, First experimental evidence for the elusive tetrahedral cations $[EP_3]^+$ (E = S, Se, Te) in the condensed phase. *Chem. Sci.* **10**, 10779–10788 (2019).

9. D. Opalka, L. V. Poluyanov, W. Domcke, Relativistic Jahn-Teller effects in the photoelectron spectra of tetrahedral P_4, As_4, Sb_4, and Bi_4. *J. Chem. Phys.* **135**, 104108 (2011).

10. P. Jerabek, G. Frenking, Comparative bonding analysis of N_2 and P_2 versus tetrahedral N_4 and P_4. *Theor. Chem. Acc.* **133**, 1447 (2014).

11. S. Urpelainen, J. Niskanen, J. A. Kettunen, M. Huttula, H. Aksela, Valence photoionization and resonant Auger decay of Sb_4 clusters at resonances below the *4d* ionization threshold. *Phys. Rev. A* **83**, 015201 (2011).

12. J. A. Kettunen, S. Urpelainen, S. Heinäsmäki, M. Huttula, Dissociation of As_4 clusters following valence photoionization and *3d* core excitation. *Phys. Rev. A* **86**, 023201 (2012).

13. S. Rayne, K. Forest, Binary mixed carbon, silicon, nitrogen, and phosphorus cubane derivatives as potential high energy materials. *Comput. Theor. Chem.* **1080**, 10–15 (2016).

14. A. Hirsch, Z. Chen, H. Jiao, Spherical aromaticity of inorganic cage molecules. *Angew. Chem. Int. Ed.* **40**, 2834–2838 (2001).

15. P. V. R. Schleyer, C. Maerker, A. Dransfeld, H. Jiao, N. J. R. van Eikema Hommes, Nucleus-independent chemical shifts: A simple and efficient aromaticity probe. *J. Am. Chem. Soc.* **118**, 6317–6318 (1996).

16. F. Cacace, G. de Petris, A. Troiani, Experimental detection of tetranitrogen. *Science* **295**, 480–481 (2002).

17. O. Kwon, P. M. Almond, M. L. McKee, Structures and reactions of P_2N_2: A hybrid of elemental N_2 and P_4? *J. Phys. Chem. A* **106**, 6864–6870 (2002).

18. L. Wang, P. L. Warburton, P. G. Mezey, A theoretical study of nitrogen-rich phosphorus nitrides $P(N_n)_m$. *J. Phys. Chem. A* **109**, 1125–1130 (2005).

19. G. A. Ozin, High-temperature gas-phase laser Raman spectroscopy: Evidence for the existence and molecular structure of the interpnictides As_3P, As_2P_2, and AsP_3 in mixtures of phosphorus and arsenic vapours and SbP_3 in mixtures of phosphorus and antimony vapours. *J. Chem. Soc. A*, 2307–2310 (1970).

20. N. A. Piro, C. C. Cummins, P_2 addition to terminal phosphide M≡P triple bonds: A rational synthesis of *cyclo*-P_3 complexes. *J. Am. Chem. Soc.* **130**, 9524–9535 (2008).

21. B. M. Cossairt, M.-C. Diawara, C. C. Cummins, Facile synthesis of AsP_3. *Science* **323**, 602–602 (2009).

22. N. A. Piro, C. C. Cummins, Tetraphosphabenzenes obtained via a triphosphacyclobutadiene intermediate. *Angew. Chem. Int. Ed.* **48**, 934–938 (2009).

23. N. A. Piro, thesis, Massachusetts Institute of Technology, Cambridge, MA (2009).

24. B. M. Cossairt, C. C. Cummins, Properties and reactivity patterns of AsP_3: An experimental and computational study of group 15 elemental molecules. *J. Am. Chem. Soc.* **131**, 15501–15511 (2009).

25. B. M. Cossairt, C. C. Cummins, A. R. Head, D. L. Lichtenberger, R. J. F. Berger, S. A. Hayes, N. W. Mitzel, G. Wu, On the molecular and electronic structures of AsP_3 and P_4. *J. Am. Chem. Soc.* **132**, 8459–8465 (2010).

26. M. Y. Riu, M. Ye, C. C. Cummins, Alleviating strain in organic molecules by incorporation of phosphorus: Synthesis of triphosphatetrahedrane. *J. Am. Chem. Soc.* **143**, 16354–16357 (2021).

27. Y. Valadbeigi, Phosphorus-doped nitrogen clusters (N_nP_m): Stable high energy density materials. *Chem. Phys. Lett.* **645**, 195–199 (2016).

28. A. M. Turner, R. I. Kaiser, Exploiting photoionization reflectron time-of-flight mass spectrometry to explore molecular mass growth processes to complex organic molecules in interstellar and solar system ice analogs. *Acc. Chem. Res.* **53**, 2791–2805 (2020).

29. C. Zhu, A. K. Eckhardt, S. Chandra, A. M. Turner, P. R. Schreiner, R. I. Kaiser, Identification of a prismatic P_3N_3 molecule formed from electron irradiated phosphine-nitrogen ices. *Nat. Commun.* **12**, 5467 (2021).

30. G. Socrates, *Infrared and Raman Characteristic Group Frequencies: Tables and Charts* (Wiley, 2004).

31. K. K. Irikura, R. D. Johnson, R. N. Kacker, R. Kessel, Uncertainties in scaling factors for ab initio vibrational zero-point energies. *J. Chem. Phys.* **130**, 114102 (2009).

32. P. Pyykkö, Additive covalent radii for single-, double-, and triple-bonded molecules and tetrahedrally bonded crystals: A summary. *J. Phys. Chem. A* **119**, 2326–2337 (2015).

33. Y. Naruse, S. Inagaki, in *Orbitals in Chemistry*, S. Inagaki, Ed. (Springer Berlin Heidelberg, 2010), pp. 265–291.

34. R. D. Bach, O. Dmitrenko, The effect of carbonyl substitution on the strain energy of small ring compounds and their six-member ring reference compounds. *J. Am. Chem. Soc.* **128**, 4598–4611 (2006).

35. H. Bock, H. Mueller, Gas-phase reactions. 44. The phosphorus $P_4 \leftrightarrow 2P_2$ equilibrium visualized. *Inorg. Chem.* **23**, 4365–4368 (1984).

36. B. M. Jones, R. I. Kaiser, Application of reflectron time-of-flight mass spectroscopy in the analysis of astrophysically relevant ices exposed to ionization radiation: Methane (CH_4) and D_4-methane (CD_4) as a case study. *J. Phys. Chem. Lett.* **4**, 1965–1971 (2013).

37. N. A. Piro, J. S. Figueroa, J. T. McKellar, C. C. Cummins, Triple-bond reactivity of diphosphorus molecules. *Science* **313**, 1276–1279 (2006).

38. A. Velian, M. Nava, M. Temprado, Y. Zhou, R. W. Field, C. C. Cummins, A retro Diels–Alder route to diphosphorus chemistry: Molecular precursor synthesis, kinetics of P_2 transfer to 1,3-dienes, and detection of P_2 by molecular beam mass spectrometry. *J. Am. Chem. Soc.* **136**, 13586–13589 (2014).

39. A. Velian, C. Cummins Christopher, Synthesis and characterization of $P_2N_3^-$: An aromatic ion composed of phosphorus and nitrogen. *Science* **348**, 1001–1004 (2015).

40. G. L. Hou, B. Chen, W. J. Transue, D. A. Hrovat, C. C. Cummins, W. T. Borden, X. B. Wang, Negative ion photoelectron spectroscopy of $P_2N_3^-$: Electron affinity and electronic structures of $P_2N_3^{\bullet}$. *Chem. Sci.* **7**, 4667–4675 (2016).

41. A. Eckhardt, M.-L. Riu, M. Ye, P. Mueller, G. Bistoni, C. Cummins, Taming phosphorus mononitride (PN) (ChemRxiv, 2021); https://doi.org/10.33774/chemrxiv-2021-zxtmf.

42. J. L. Martinez, S. A. Lutz, D. M. Beagan, X. Gao, M. Pink, C. H. Chen, V. Carta, P. Moenne-Loccoz, J. M. Smith, Stabilization of the dinitrogen analogue, phosphorus nitride. *ACS Cent. Sci.* **6**, 1572–1577 (2020).

43. A. M. Turner, M. J. Abplanalp, S. Y. Chen, Y. T. Chen, A. H. Chang, R. I. Kaiser, A photoionization mass spectroscopic study on the formation of phosphanes in low temperature phosphine ices. *Phys. Chem. Chem. Phys.* **17**, 27281–27291 (2015).

44. R. Luna, M. Á. Satorre, M. Domingo, C. Millán, C. Santonja, Density and refractive index of binary CH_4, N_2 and CO_2 ice mixtures. *Icarus* **221**, 186–191 (2012).

45. D. Drouin, A. R. Couture, D. Joly, X. Tastet, V. Aimez, R. Gauvin, CASINO V2.42—A fast and easy-to-use modeling tool for scanning electron microscopy and microanalysis users. *Scanning* **29**, 92–101 (2007).

46. M. J. Frisch, G. W. Trucks, H. B. Schlegel, G. E. Scuseria, M. A. Robb, J. R. Cheeseman, G. Scalmani, V. Barone, G. A. Petersson, H. Nakatsuji, X. Li, M. Caricato, A. V. Marenich, J. Bloino, B. G. Janesko, R. Gomperts, B. Mennucci, H. P. Hratchian, J. V. Ortiz, A. F. Izmaylov, J. L. Sonnenberg, Williams, F. Ding, F. Lipparini, F. Egidi, J. Goings, B. Peng, A. Petrone, T. Henderson, D. Ranasinghe, V. G. Zakrzewski, J. Gao, N. Rega, G. Zheng, W. Liang, M. Hada, M. Ehara, K. Toyota, R. Fukuda, J. Hasegawa, M. Ishida, T. Nakajima, Y. Honda, O. Kitao, H. Nakai, T. Vreven, K. Throssell, J. A. Montgomery Jr., J. E. Peralta, F. Ogliaro, M. J. Bearpark, J. J. Heyd, E. N. Brothers, K. N. Kudin, V. N. Staroverov, T. A. Keith, R. Kobayashi, J. Normand, K. Raghavachari, A. P. Rendell, J. C. Burant, S. S. Iyengar, J. Tomasi, M. Cossi, J. M. Millam, M. Klene, C. Adamo, R. Cammi, J. W. Ochterski, R. L. Martin, K. Morokuma, O. Farkas, J. B. Foresman, D. J. Fox, *Gaussian 16 Rev. C.01* (2016).

47. A. D. Becke, Density-functional exchange-energy approximation with correct asymptotic behavior. *Phys. Rev. A* **38**, 3098–3100 (1988).

48. C. Lee, W. Yang, R. G. Parr, Development of the colle-salvetti correlation-energy formula into a functional of the electron density. *Phys. Rev. B* **37**, 785–789 (1988).

49. A. D. Becke, Density-functional thermochemistry. III. The role of exact exchange. *J. Chem. Phys.* **98**, 5648–5652 (1993).

50. T. H. Dunning, Gaussian basis sets for use in correlated molecular calculations. I. The atoms boron through neon and hydrogen. *J. Chem. Phys.* **90**, 1007–1023 (1989).

51. R. J. Bartlett, J. D. Watts, S. A. Kucharski, J. Noga, Non-iterative fifth-order triple and quadruple excitation energy corrections in correlated methods. *Chem. Phys. Lett.* **165**, 513–522 (1990).

52. J. Čížek, On the correlation problem in atomic and molecular systems. Calculation of wavefunction components in ursell-type expansion using quantum-field theoretical methods. *J. Chem. Phys.* **45**, 4256–4266 (1966).

53. K. Raghavachari, Electron correlation techniques in quantum chemistry: Recent advances. *Annu. Rev. Phys. Chem.* **42**, 615–642 (1991).

54. J. F. Stanton, Why CCSD(T) works: A different perspective. *Chem. Phys. Lett.* **281**, 130–134 (1997).

55. K. A. Peterson, D. E. Woon, T. H. Dunning, Benchmark calculations with correlated molecular wave functions. IV. The classical barrier height of the $H+H_2 \rightarrow H_2+H$ reaction. *J. Chem. Phys.* **100**, 7410–7415 (1994).

56. J. A. Montgomery, M. J. Frisch, J. W. Ochterski, G. A. Petersson, A complete basis set model chemistry. VII. Use of the minimum population localization method. *J. Chem. Phys.* **112**, 6532–6542 (2000).

57. S. G. Lias, Ionization energy evaluation, in *NIST Chemistry WebBook* (NIST Standard Reference Database Number 69, 2022); https://doi.org/10.18434/T4D303.

58. D. C. Frost, S. T. Lee, C. A. McDowell, The photoelectron spectrum of HCP and comments on the first photoelectron band of HCN. *Chem. Phys. Lett.* **23**, 472–475 (1973).

59. A. M. Turner, S. Chandra, R. C. Fortenberry, R. I. Kaiser, A photoionization reflectron time-of-flight mass spectrometric study on the detection of ethynamine ($HCCNH_2$) and 2H-azirine (c-H_2 CCHN). *ChemPhysChem* **22**, 985–994 (2021).